

Article

Structure and Photoelectrical Properties of Natural Photoactive Dyes for Solar Cells

Qian Liu ¹, Nan Gao ², Dejiang Liu ^{3,4}, Jinglin Liu ^{3,*} and Yuanzuo Li ^{2,*} ¹ Department of Applied Physics, Xi'an University of Technology, Xi'an 710054, China; liuqian@xaut.edu.cn² College of Science, Northeast Forestry University, Harbin 150040, China; nan_g@nefu.edu.cn³ Department of Physics, Jiamusi University, Jiamusi 154001, China; liudejiang2004@163.com⁴ Life Science College, Jiamusi University, Jiamusi 154007, China

* Correspondence: jinglinliujms@yeah.net (J.L.); yzli@nefu.edu.cn (Y.L.)

Received: 29 July 2018; Accepted: 13 September 2018; Published: 19 September 2018



Abstract: A series of natural photoactive dyes, named as D1–D6 were successfully extracted from six kinds of plant leaves for solar cells. The photoelectrical properties of dyes were measured via UV-Vis absorption spectra, cyclic voltammetry as well as photovoltaic measurement. To theoretically reveal the experimental phenomena, the chlorophyll was selected as the reference dye, where the ground and excited state properties of chlorophyll were calculated via density functional theory (DFT) and time-dependent density functional theory (TD-DFT). The experimental results show that the absorption peaks of those dyes are mainly distributed in the visible light regions of 400–420 nm and 650–700 nm, which are consistent with the absorption spectrum of chlorophyll. The photoelectrical conversion efficiencies of the solar cells sensitized by the six kinds of natural dyes are in the order of D1 > D4 > D2 > D5 > D6 > D3. The dye D1 performance exhibits the highest photoelectrical conversion efficiency of 1.08% among the investigated six natural dyes, with an open circuit voltage of 0.58 V, a short-circuit current density of 2.64 mA cm⁻² and a fill factor of 0.70.

Keywords: natural photo-active dyes; UV-Vis absorption spectra; density functional theory (DFT); Dye-sensitized solar cells (DSSCs)

1. Introduction

With the development and utilization of renewable energy, much works have been paid attention to the devices converting solar energy into electrical energy, among which the dye-sensitized solar cells (DSSCs) with its characteristics of low fabrication costs, environmentally friendly components and relatively high photoelectrical conversion efficiency (PCE) have received wide attention [1–5]. In 1991, Regan and Gratzel [6] created the DSSCs with overall PCE yield of 7.1–7.9% in simulated solar light from low- to medium-purity materials by low-cost process. DSSCs are mainly composed of a light absorbing photoanode, dyes, an electrolyte containing redox couple and a counter electrode [7]. It is remarkable that the dyes play a crucial role in DSSCs because firstly they absorb sunlight [8], followed by injection of the excited electron into semiconductor. In addition to the use of dyes containing metal elements [9–11], the metal-free organic dyes have been widely applied to the field of DSSCs [12–19]. However, the shortcomings of high cost, environmental pollution and also expensive chemical synthesis process are worth the attention of the researchers [20]. Fortunately, researchers have found that the application of natural dyes extracted from the plant flowers petals, leaves, roots in the DSSCs, also producing a considerable PCE [20–33], which has opened up a friend way for the conversion of solar energy into electricity. For example, Hosseinneshad et al., used some natural dyes as photosensitizers (extracted from *Celosia Cristata*, Saffron, *Cynoglossum*, and eggplant peel) [21], in which PCE is found to be 1.38% (*Celosia Cristata*). Five different natural dyes with various anchoring

groups have been studied from various plants and used them as photo-sensitizers in DSSC [22], showing possess better absorption at 300–550 nm. Hamadani et al. [23] used a series of natural dye extracted from plants for the DSSCs. Because Delphinidin was the main pigment of *C. ajacis*, interaction between the hydroxyl groups of the Delphinidin and the TiO_2 surface was very efficient, and this sensitizer owned the best photovoltaic performance among all the natural dyes. It was interesting that Maiaugree and co-workers [24] used carbonized mangosteen peel and mangosteen peel dye as a natural counter electrode and a natural photo-sensitizer for DSSC application, respectively; they found a distinctive mesoporous honeycomb-like carbon structure with a rough nanoscale surface in carbonized mangosteen peels, resulting in the highest PCE (2.63%) when using carbonized mangosteen peel and an organic disulfide/thiolate (T_2/T^-) electrolyte. Since the first report on Chlorophyll (Chl) and its derivatives as sensitizers in DSSCs [32], the greater sensitizer ability of Chl derivatives with respect to the pure untreated chlorophyll a was evidenced, which result can be explained considering the fact that the low attitude of this natural pigment should be efficiently absorbed on TiO_2 layer when dissolved in some solvent (ethanol, acetone, pyridine, etc.). Generally, the dye extracted from natural species are not pure chlorophyll but natural compounds derived by chlorophyll a and b. Recent study found the copper-Chle6 achieving the following parameters: FF of 0.65, V_{OC} of 438 mV and PCE of 1.81% [33]. There are also several ways to improvement of solar cell performances by photoanodes modification, such as the photoanodes modification based on H- TiO_2 NPs scattering layer [34] and indium doped ZnO photoanode [35].

Recently, the theoretical method based on quantum chemistry calculation has provided the valuable reference for predicting the relationship between the structure and photoelectrical properties of molecules [36–40]. Qin et al. [41] reported a theoretical study of the betalain pigments using density functional theory (DFT) and time-dependent density functional theory (TD-DFT), and the results indicated that the lowest unoccupied molecular orbital (LUMO) had a close spatial proximity to bound TiO_2 , assuming that betalain binding occurred through the two carboxylic groups on the dihydropyridine ring. Khadtare et al. [42] analyzed the spectral features of lawsone (2-hydroxy-1,4-naphthoquinone), an active component of the natural dye henna in ethanol by using experimental and computational methods; the study showed that the 1,4-naphthoquinone classes of compounds can provide the basis for the design of novel compounds for DSSCs to enhance its efficiency. Charge transfer enhancement in DSSCs was reported by changing the electron donor of the famous porphyrin-based sensitizer YD2-o-C8 [43].

In this work, six natural dyes, named as D1, D2, D3, D4, D5 and D6, were successfully extracted from the leaves of *Euodia meliaefolia* (Hance) Benth, *Matteuccia struthiopteris* (L.) Todaro, *Corylus heterophylla* Fisch, *Filipendula intermedia*, *Pteridium aquilinum* var. *latiusculum* and *Populus L* (see Figure 1), respectively. The optical and electrical properties of the dyes applied in DSSCs were measured via UV-Vis absorption spectra and cyclic voltammetry. To compare with the experimental results, the chlorophyll was selected as the reference molecule, and the ground and excited state properties of chlorophyll were calculated via DFT and TD-DFT methods, respectively. The obtained results indicate the DSSC sensitized by the dye D1 exhibits the highest PCE of 1.08% among the investigated six natural dyes, with an open circuit voltage (V_{OC}) of 0.58 V, a short-circuit current density (J_{SC}) of 2.64 mA cm^{-2} and a fill factor (FF) of 0.70.

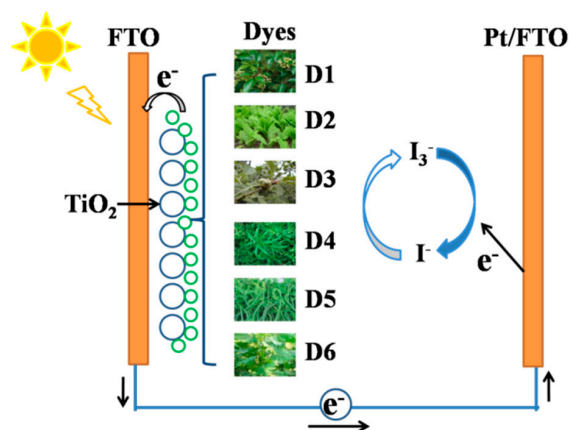


Figure 1. Basic working principle of DSSC, which mainly contains four parts: photoanode, natural dyes, electrolyte containing redox couple and counter electrode, where photosensitive layer using the dyes (D1–D6) were extracted from the leaves.

2. Methods

The fresh leaves of the six plants were selected and placed into a vacuum drying oven maintaining 70 °C to remove moisture. The dried leaves were pulverized into powder in a mortar and weighed 1 g powder, and then mixed 20 mL ethanol with the power. After keeping the admixture away from the light in a brown jar for a week, the efficient natural dyes were obtained through a simple filtering process. The structure of prepared DSSC was mainly made of TiO₂ photo-anode, dye and electrolyte. The specific production process is as our previous works [16]: (a) the TiO₂ electrode was prepared through adding 10 mL isopropyl titanate into water, and keeping the hydrolysis for 3 h, and then adding nitric acid and acetate into the solution, and placing in an environment of 80 °C; the mixed solution was stirred until it became transparent blue; later, the hydrothermal reaction was executed at 200 °C for 12 h. After cooling, spin steaming, centrifuging, terpeneol ethyl and cellulose were added into the ball grinder; the paste were prepared completely by ball mill, rotary steam and three roll. (b) the screen printing technology was adopted to print the TiO₂ paste to the clean surface of a conductive glass, and the active area of TiO₂ photo-anode was 0.16 cm²; after ethanol bathing and drying, the TiO₂ photo-anode was sintered, and then treated in TiCl₄ solvent. After this, the photo-anode was sintered again. In the later process, the photo-anode was immediately removed after the natural cooling to 80 °C, and the photo-anode was soaked in the natural dye without light for 24 h. (c) the photo-anode and the platinum plating counter electrode were fitted together into the cell, and in the middle of the two electrodes, the electrolyte solution (including 0.5 M LiI, 0.05 M I₂ TBP, GUSCN) was added. The SEM image of thin film of TiO₂ nanoparticles was shown in Figure 2, where the area of TiO₂ film was 16 mm² and thickness of the TiO₂ anode layer was about 16–18 μm; here, the characteristic of void and honeycomb of TiO₂ anode layer is benefit for enhancing the adsorption of dyes.

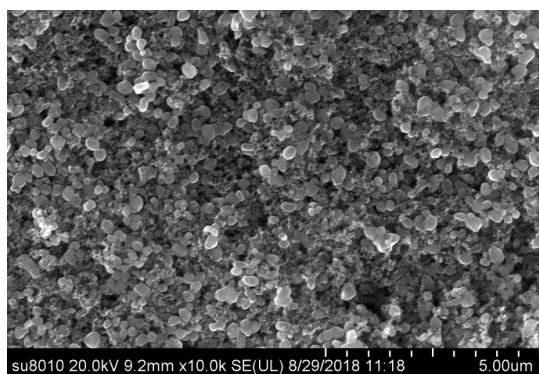


Figure 2. SEM micrographs of the TiO₂ nanoparticles on the glass.

UV-Vis spectra of dye solutions and dye adsorbed on TiO₂ photo-anodes were measured with TU-1900 spectrometer (Beijing Purkinje General Instrument Co., Ltd., Beijing, China). Cyclic voltammetry properties were performed by using CH Instruments CHI832C Electrochemical Workstation (Shanghai Chenhua Instrument Co., Ltd., Shanghai, China). The redox potentials of the dyes were measured in ethanol solvent. The scan range was between -1000 mV and $+1000$ mV, and the initial scan potential was -1000 mV, at a scan rate of 50 mV/s. Here, a glassy carbon working electrode, platinum counter electrode and Ag/AgCl reference electrode were used to form electrode system, where 0.1 M KNO₃ was used as the supporting electrolyte [44]. Solar energy conversion efficiency measurements were completed with a solar simulation instrument (PEC-L15, Peccell Technologies, Inc., Yokohama, Japan), and light intensity was adjusted via a reference standard Si-solar solar cell at 1 sun light intensity of 100 mW cm⁻².

Compared with experiment, the chlorophyll was selected as the reference dye in theory, and the ground state structure of chlorophyll a was optimized by using DFT [45], with B3LYP [46–48] functional at 6-31G(d) basis set. On the base of optimized ground state structure, the excited state properties of chlorophyll were calculated via TD-DFT [49] with different functionals, containing Cam-B3LYP, MPW1PW91 and PBEPBE [50–53] at 6-31G(d) basis set. By comparing the obtained theoretical and experimental results, the calculated absorption spectrum of chlorophyll by using the PBEPBE functional was well consistent with the experimental results. Therefore, we selected the theoretical results calculated by using PBEPBE functional to reveal the experimental results. The ethanol was selected as the solvent, and all calculations in solvent adopted the Conductor-like PCM (C-PCM) model [54]. DFT calculations was used to study photosensitizing features [55] and photophysical properties of expanded bacteriochlorins [56], where micromechanism of photosensitizing nature was revealed with DFT calculations. In addition, the three-dimensional (3D) real-space analysis method was used to describe the charge transfer process in the excited states [57–60]. All calculations were performed using Gaussian 09 package [61].

3. Results and Discussion

3.1. UV-Vis Absorption Spectra in Experiment and Theory

The UV-Vis absorption spectra of the dyes in ethanol and dye adsorbed on TiO₂ photo-anodes were measured, and the corresponding absorption spectra are presented in Figure 3a,b. The detected absorption peaks corresponding to the isolated dyes and dyes adsorbed on TiO₂ are listed in Table 1 in detail. As shown in Figure 3a, the absorption spectra of those six kinds of dyes have similar appearance, in which the absorption peaks are mainly distributed in the visible light regions of 400 – 420 nm and 650 – 700 nm. It is worth noting that all the absorption spectra of the investigated dyes have the characteristics of double peaks, which are advantageous to the absorption of dyes on the sun light. As listed in Table 1, the two absorption peaks of the six dyes are focused on about 412 nm and 664 nm. The absorption spectra of the dyes investigated in the present work are consistent with the absorption spectrum of chlorophyll [62,63]. In addition, the absorption spectra of dyes adsorbed on TiO₂ photo-anode are shown in Figure 3b, and the corresponding absorption peaks are listed in Table 1. As listed in Table 1, the absorption peaks in the region of 650 – 700 nm exhibit different extent of red-shifts compared with that of the isolated dyes, in which the red-shift values are 7.5 nm, 10 nm, 6.5 nm, 29.5 nm, 7.5 nm and 6.5 nm for D1, D2, D3, D4, D5 and D6, respectively.

Table 1. Absorption peaks of isolated dyes and dye adsorbed on TiO₂.

Dye	Absorption Peaks (nm)	Dye/TiO ₂	Absorption Peaks (nm)
D1	416.0, 664.0	D1/TiO ₂	416.5, 671.5
D2	419.5, 658.5	D2/TiO ₂	421.5, 668.5
D3	412.5, 663.5	D3/TiO ₂	416.5, 670.0
D4	411.5, 665.5	D4/TiO ₂	695.0
D5	413.5, 664.0	D5/TiO ₂	413.5, 671.5
D6	412.0, 665.0	D6/TiO ₂	416.5, 671.5

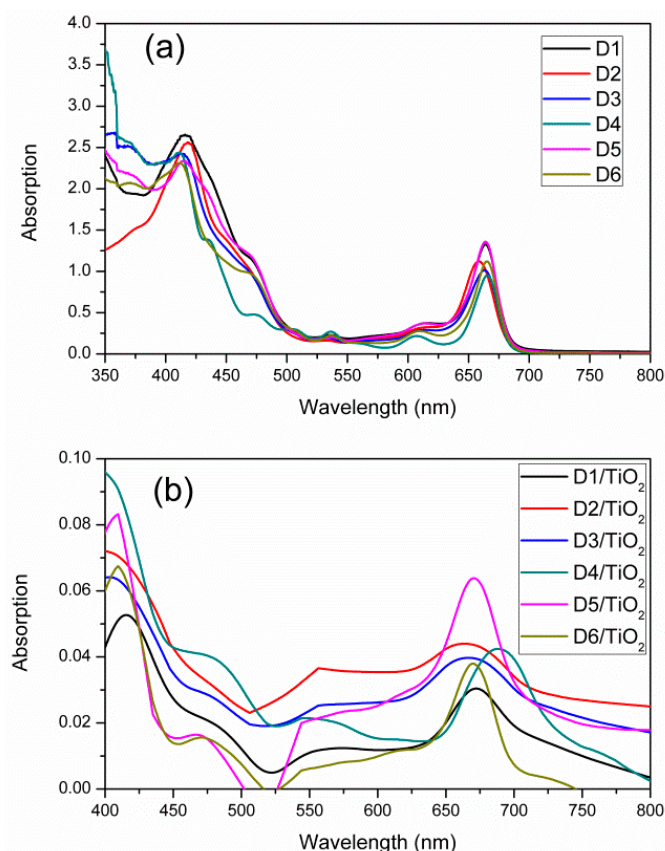


Figure 3. Absorption spectra of (a) isolated dyes and (b) dye adsorbed on TiO₂.

To compare with the experimental results, the excited state properties of chlorophyll was investigated via TD-DFT method with different functionals at 6-31G(d) basis set based on the optimized ground state structure of chlorophyll, due to the fact that chlorophyll accounts for the largest proportion in the green plant leaves. The simulated absorption spectra of chlorophyll by using different functionals are presented in Figure 4, and the corresponding absorption peaks are listed in Table 2. Combined with the results of Figure 4 and Table 2, it can be seen that the simulated absorption spectrum of chlorophyll by using PBEPBE functional is more consistent with the experimental results; so we analyze the excited state properties of chlorophyll based on the results calculated by the PBEPBE functional. The calculated excitation energies, absorption peaks, electronic transition configurations and corresponding oscillator strengths of the first ten excited states are listed in Table 3. As listed in Table 3, the excited state S8 corresponds to the first maximum absorption peak 439.66 nm with the oscillator strength of 0.3846, which is mainly formed by the electrons transition from HOMO – 1 to LUMO + 1. In addition, the excited state S1 corresponds to the second maximum absorption peak at 621.44 nm with the oscillator strength of 0.3042, which is mainly originated from the electrons transition from HOMO to LUMO. Moreover, the excited state S7 corresponds to the third maximum absorption peak at 456.17 nm (the oscillator strength of 0.2823), which mainly comes from the electrons transition from HOMO to LUMO + 1.

Table 2. Calculated absorption peaks and corresponding oscillator strengths (in bracket) of chlorophyll via TD-DFT method with different functionals at 6-31G(d).

Peak	Cam-B3LYP	MPW1PW91	PBEPBE
$\lambda_{\max 1}$ ^a	376.57 (0.9972)	375.28 (0.8763)	439.66 (0.3846)
$\lambda_{\max 2}$ ^b	602.89 (0.3746)	586.59 (0.3816)	621.44 (0.3042)

^a corresponds to the first absorption peak; ^b corresponds to the second absorption peak.

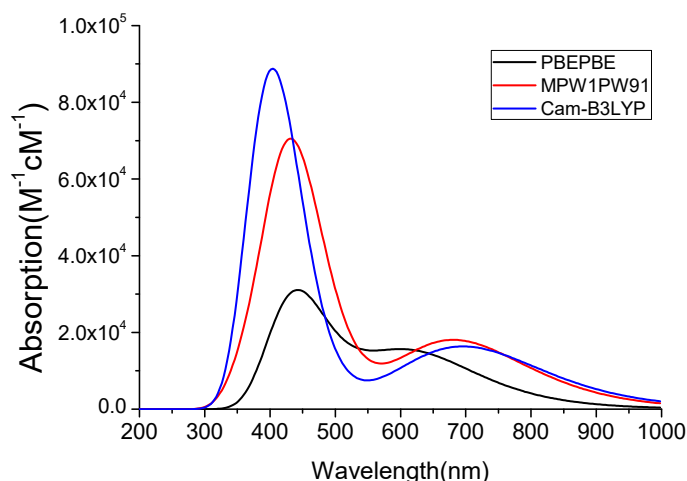


Figure 4. Simulated absorption spectra of chlorophyll in ethanol via different functionals with 6-31G(d) basis set.

Table 3. Calculated excitation energies (E , eV), absorption peaks (λ_{abs} , nm), electronic transition configurations and corresponding oscillator strengths (f) of chlorophyll a in ethanol by using TD-DFT//PBE/PBE/6-31G(d) method.

State	E (eV)	λ_{abs} (nm)	Contribution MO	Strength f
S1	1.9951	621.44	(0.65673)H→L	0.3042
S2	2.0275	611.51	(0.63801)H-1→L	0.0561
S3	2.3641	524.44	(0.68996)H-2→L	0.0027
S4	2.4662	502.73	(0.65897)H-4→L	0.0010
S5	2.4969	496.56	(0.65411)H-3→L	0.0086
S6	2.6161	473.93	(0.70631)H-5→L	0.0008
S7	2.7179	456.17	(0.46269)H→L + 1	0.2823
S8	2.8200	439.66	(0.40417)H-1→L + 1	0.3846
S9	2.9989	413.43	(0.61479)H-7→L	0.0555
S10	3.0548	405.87	(0.56616)H-6→L	0.0847

For Dye/TiO₂ system, calculated absorption information has been listed in supporting materials (Table S1). Calculated absorption peaks is found to be 705.79 nm corresponding to the sixth excited state, which make red-shifted in comparison with the isolated dye in solvent. The closed strength is located in 657.66 nm, which is in ninth excited state. Charge different density shows the distribution of charge during light absorption, which is shown in Figure 5. As shown, for the sixth excited state red electron is move into the semiconductor and hole is resided in the porphyrin ring. Hence this state is charge transfer (CT) state, and similar CT process can be found in ninth excited state, and more migration of electrons into semiconductor is benefit for electron transport for external circuit.

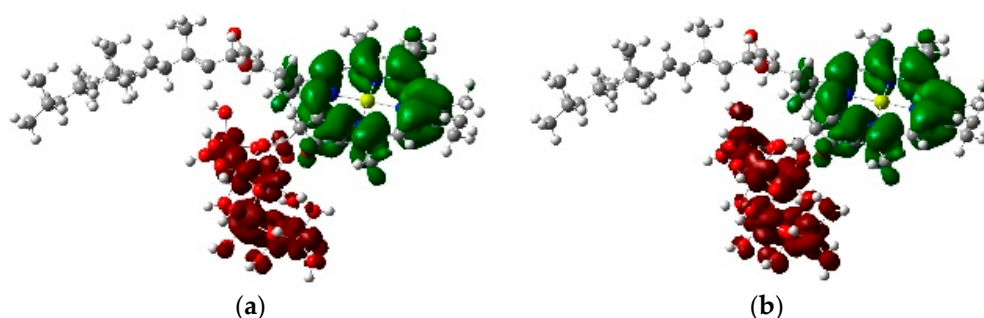


Figure 5. Charge difference density (CDD) for chlorophyll/TiO₂. (a) S6; (b) S9.

3.2. Electrochemical Properties

The thermodynamic feasibility of electron injection from the excited dye molecule to the TiO_2 conduction band and dye regeneration utilizing electrolyte can be investigated through the research on the electrochemical properties of the dyes [64,65]. Herein, the electrochemical properties of the six kinds of natural dyes were studied via cyclic voltammetry measurement in the ethanol solvent, adopting 0.1 M KNO_3 as the supporting electrolyte. The measured cyclic voltammetry curves of the six dyes are exhibited in Figure 6, and the onset oxidation potentials of the dyes obtained from the curves are listed in Table 4. As listed in Table 4, the onset oxidation potentials of the six dyes are 0.34 V, 0.19 V, -0.07 V, 0.07 V, 0.11 V and 0.10 V for D1, D2, D3, D4, D5 and D6, respectively. From the previous report [66], it can be known that the HOMO energy can be obtained by the onset oxidation potential of dye, when an Ag/AgCl electrode is used as the reference electrode; the HOMO energy can be calculated via the following equation: $\text{HOMO} = -e(E_{\text{OX}} + 4.40)$ (eV), where E_{OX} stands for the onset oxidation potential of dye. The calculated HOMO energies of the six dyes are listed in Table 4, which shows that the HOMO energies of the six dyes are -4.74 eV, -4.59 eV, -4.33 eV, -4.47 eV, -4.51 eV and -4.50 eV for D1, D2, D3, D4, D5 and D6, respectively. In terms of the work of Tian et al. [67], the dye with strong donating ability will exhibit the more negative HOMO level. Therefore, it can be concluded from the obtained HOMO energies of these dyes that the electron donating ability of these dyes in the order of $\text{D1} > \text{D2} > \text{D5} > \text{D6} > \text{D4} > \text{D3}$. Their LUMOs are higher than that are higher than semiconductor band (-4.0 eV), meaning possible occurrence of electron injection for studied systems. Furthermore, the lowest HOMO can enhance the ability of dye regeneration because the larger driving force of dye regeneration between dye and electrolytic, which is contributed to the J_{SC} .

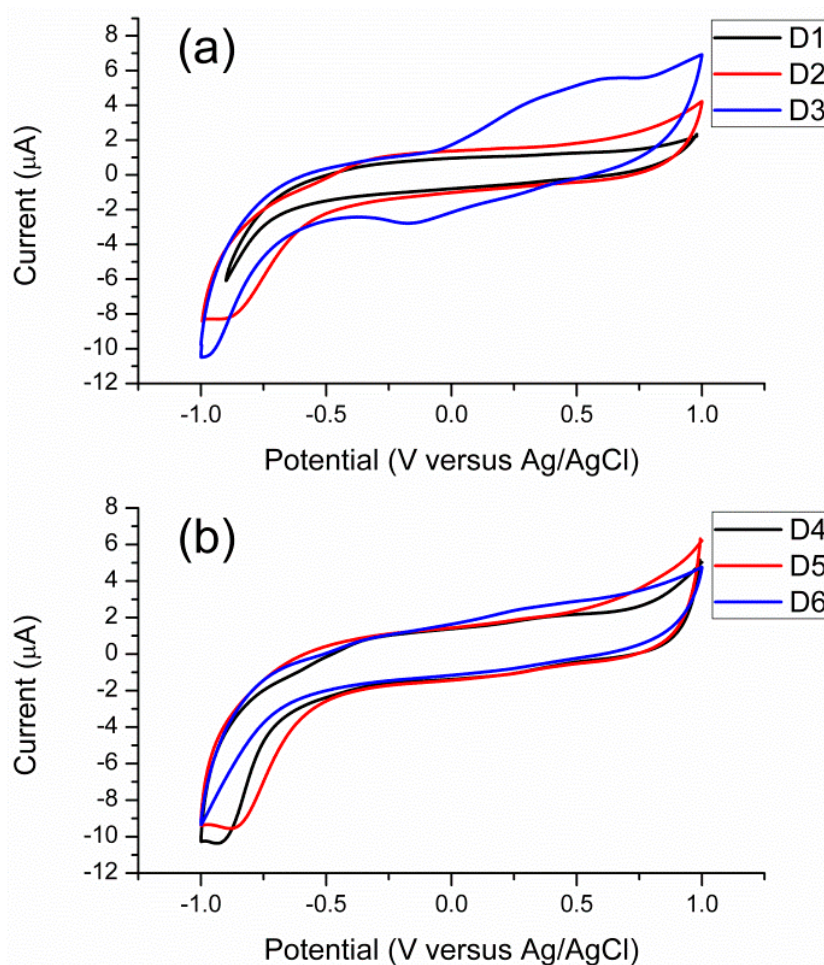


Figure 6. Cyclic voltammograms of the six natural dyes. (a) dyes D1–D3; (b) dyes D4–D6.

Table 4. Electrochemical properties of the six natural dyes.

Dye	E _{OX} (V) ^a	HOMO (eV)	LUMO ^b (eV)	Dye	E _{OX} (V) ^a	HOMO (eV)	LUMO (eV)
D1	0.34	−4.74	−2.873	D4	0.07	−4.47	−2.607
D2	0.19	−4.59	−2.707	D5	0.11	−4.51	−2.643
D3	−0.07	−4.33	−2.461	D6	0.10	−4.50	−2.636

^a The onset oxidation potential of the dye; ^b estimation from HOMO and excitation energy [68].

3.3. Photoelectric Properties of DSSCs

The photoelectrical conversion efficiency (η) of the DSSC is defined via the following equation [69]:

$$\eta = \frac{J_{SC} \times V_{OC} \times FF}{P_{in}} \quad (1)$$

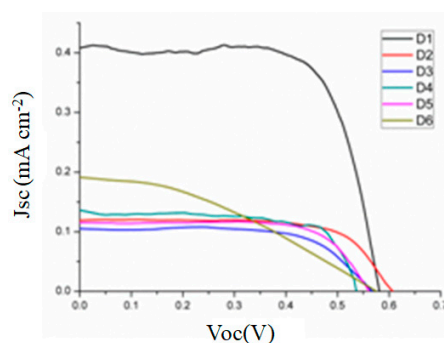
where J_{SC} is the short-circuit current density, V_{OC} represents the open circuit voltage, FF is the fill factor, and P_{in} is the intensity of the incident light, in which the J_{SC} , V_{OC} and FF are only obtained through the experiment.

The fill factor (FF) is defined as the ratio of the maximum power obtained from the DSSC and the theoretical maximum power, which can be understood by the following equation:

$$FF = \frac{I_m \times V_m}{J_{SC} \times V_{OC}} \quad (2)$$

where I_m and V_m represent the current and voltage related to the maximum power, respectively.

The measured current-voltage curves of the fabricated DSSCs sensitized by the six kinds of natural dyes are shown in Figure 7, and the photovoltaic parameters of the DSSCs, containing V_{OC} , J_{SC} , FF and η are listed in Table 5. It can be found from Table 5 that the PCE of the DSSCs sensitized by the six kinds of natural dyes are in the order of D1 > D4 > D2 > D5 > D6 > D3, in which the DSSC sensitized by the dye D1 exhibit the highest PCE of 1.08%, with V_{OC} of 0.58 V, J_{SC} of 2.64 mA cm^{−2} and FF of 0.70. It is worth noting that the DSSC sensitized by the dye D1 possesses the highest J_{SC} among the investigated DSSCs, which can be promoted by the improved ability of dye regeneration can promote.

**Figure 7.** Current-Voltage curves of DSSCs sensitized with the six natural dyes.**Table 5.** Measured photovoltaic parameters of the fabricated DSSCs.

DSSCs	V _{OC} (V)	J _{SC} mA cm ^{−2}	FF	η (%)
D1	0.58	2.64	0.70	1.08
D2	0.60	0.75	0.72	0.32
D3	0.56	0.68	0.69	0.26
D4	0.54	0.87	0.74	0.34
D5	0.56	0.74	0.73	0.30
D6	0.57	1.25	0.37	0.27

4. Conclusions

In this work, a series of natural dyes (D1, D2, D3, D4, D5 and D6) were successfully extracted from six kinds of plant leaves, and their optical and electrical properties were measured via UV-Vis absorption spectra and cyclic voltammetry. To reveal the experimental phenomena, the chlorophyll was selected as the reference molecule, and the DFT and TDDFT methods were adopted to calculate the ground and excited state properties of chlorophyll. The experimental results indicate that the absorption spectra of the six dyes exhibit two absorption bands in the visible light region of 400.0–420.0 nm and 650.0–700.0 nm, and the DSSC sensitized by the dye D1 exhibits the highest PCE of 1.08% among the investigated six natural dyes, with V_{OC} of 0.58 V, J_{SC} of 2.64 mA cm⁻² and FF of 0.70. The high HOMO energy levels of D1 can be contributed to the highest J_{SC} and further affect the photoelectric properties. In addition, the theoretical results imply that the excited states corresponding to the absorption peaks about 412 nm and 664 nm are mainly derived from electron transition of HOMO – 1 to LUMO + 1 and HOMO to LUMO, respectively. There exists charge transfer (CT) state, where electron is transferred into semiconductor during photoexcitation.

Supplementary Materials: Supplementary materials can be found at <http://www.mdpi.com/2076-3417/8/9/1697/s1>.

Author Contributions: Conceptualization, J.L. and Y.L.; Funding acquisition, Q.L. and Y.L.; Investigation and data analysis, Q.L., N.G. and D.L.; Software, N.G. and Y.L.; Writing—original draft, Q.L.; Writing—review & editing, Y.L. and J.L.

Funding: This work was supported by the National Natural Science Foundation of China (Grant numbers: 11404055, 61675165 and 11304135).

Conflicts of Interest: The authors declare no conflict of interest.

References

1. O'Regan, B.C.; Durrant, J.R. Kinetic and energetic paradigms for dye-sensitized solar cells: Moving from the ideal to the real. *Acc. Chem. Res.* **2009**, *42*, 1799–1808. [[CrossRef](#)]
2. Haid, S.; Marszalek, M.; Mishra, A.; Wielopolski, M.; Teuscher, J.; Moser, J.E.; Humphry-Baker, R.; Zakeeruddin, S.M.; Grätzel, M.; Bäuerle, P. Significant improvement of dye-sensitized solar cell performance by small structural modification in π -conjugated donor-acceptor dyes. *Adv. Funct. Mater.* **2012**, *22*, 1291–1302. [[CrossRef](#)]
3. Hua, Y.; Chang, S.; Huang, D.D.; Zhou, X.; Zhu, X.J.; Zhao, J.Z.; Chen, T.; Wong, W.Y.; Wong, W.K. Significant improvement of dye-sensitized solar cell performance using simple phenothiazine-based dyes. *Chem. Mater.* **2013**, *25*, 2146–2153. [[CrossRef](#)]
4. Yun, S.N.; Hagfeldt, A.; Ma, T.L. Pt-free counter electrode for dye-sensitized solar cells with high Efficiency. *Adv. Mater.* **2014**, *26*, 6210–6237. [[CrossRef](#)] [[PubMed](#)]
5. Zhou, N.J.; Prabakaran, K.; Lee, B.; Chang, S.H.; Harutyunyan, B.; Guo, P.J.; Butler, M.R.; Timalina, A.; Bedzyk, M.J.; Ratner, M.A.; et al. Metal-free tetrathienoacene sensitizers for high-performance dye-sensitized solar cells. *J. Am. Chem. Soc.* **2015**, *137*, 4414–4423. [[CrossRef](#)] [[PubMed](#)]
6. O'Regan, B.; Grätzel, M. A low-cost, high-efficiency solar cell based on dye-sensitized colloidal TiO₂ films. *Nature* **1991**, *353*, 737–740. [[CrossRef](#)]
7. Roslan, N.; Ya'acob, M.E.; Radzi, M.A.M.; Hashimoto, Y.; Jamaludin, D.; Chen, G. Dye sensitized solar cell (DSSC) greenhouse shading: New insights for solar radiation manipulation. *Renew. Sustain. Energy Rev.* **2018**, *92*, 171–186. [[CrossRef](#)]
8. Carlo, G.D.; Biroli, A.O.; Tessore, F.; Caramori, S.; Pizzotti, M. β -Substituted ZnII porphyrins as dyes for DSSC: A possible approach to photovoltaic windows. *Coord. Chem. Rev.* **2018**, *358*, 153–177. [[CrossRef](#)]
9. Bahers, T.L.; Bremond, E.; Ciofini, I.; Adamo, C. The nature of vertical excited states of dyes containing metals for DSSC applications: Insights from TD-DFT and density based indexes. *Phys. Chem. Chem. Phys.* **2014**, *16*, 14435–14444. [[CrossRef](#)] [[PubMed](#)]

10. Wei, L.G.; Na, Y.; Yang, Y.L.; Fan, R.Q.; Wang, P.; Li, L. Efficiency of ruthenium dye sensitized solar cells enhanced by 2,6-bis[1-(phenylimino)ethyl]pyridine as a co-sensitizer containing methyl substituents on its phenyl rings. *Phys. Chem. Chem. Phys.* **2015**, *17*, 1273–1280. [[CrossRef](#)] [[PubMed](#)]
11. Nosheen, E.; Shah, S.M.; Hussain, H.; Murtaza, G. Photo-sensitization of ZnS nanoparticles with renowned ruthenium dyes N3, N719 and Z907 for application in solid state dye sensitized solar cells: A comparative study. *J. Photochem. Photobiol. B Biol.* **2016**, *162*, 583–591. [[CrossRef](#)] [[PubMed](#)]
12. Zeng, W.D.; Cao, Y.M.; Bai, Y.; Wang, Y.H.; Shi, Y.S.; Zhang, M.; Wang, F.F.; Pan, C.Y.; Wang, P. Efficient dye-sensitized solar cells with an organic photosensitizer featuring orderly conjugated ethylenedioxythiophene and dithienosilole blocks. *Chem. Mater.* **2010**, *22*, 1915–1925. [[CrossRef](#)]
13. Chen, C.J.; Liao, J.Y.; Chi, Z.G.; Xu, B.J.; Zhang, X.Q.; Kuang, D.B.; Zhang, Y.; Liu, S.W.; Xu, J.R. Metal-free organic dyes derived from triphenylethylene for dye-sensitized solar cells: Tuning of the performance by phenothiazine and carbazole. *J. Mater. Chem.* **2012**, *22*, 8994–9005. [[CrossRef](#)]
14. Venkateswararao, A.; Thomas, K.R.J.; Lee, C.P.; Li, C.T.; Ho, K.C. Organic dyes containing carbazole as donor and π -linker: Optical, electrochemical, and photovoltaic properties. *ACS Appl. Mater. Interfaces* **2014**, *6*, 2528–2539. [[CrossRef](#)] [[PubMed](#)]
15. Narayanaswamy, K.; Swetha, T.; Kapil, G.; Pandey, S.S.; Hayase, S.; Singh, S.P. Simple metal-free dyes derived from triphenylamine for dssc: A comparative study of two different anchoring group. *Electrochim. Acta* **2015**, *169*, 256–263. [[CrossRef](#)]
16. Sun, C.; Li, Y.; Song, P.; Ma, F. An experimental and theoretical investigation of the electronic structures and photoelectrical properties of ethyl red and carminic acid for dssc application. *Materials* **2016**, *9*, 813. [[CrossRef](#)] [[PubMed](#)]
17. Mandal, S.; Kushwaha, S.; Mukkamala, R.; Siripina, V.K.; Aidhen, I.S.; Rajakumar, B.; Kothandaraman, R. Metal-free bipolar/octupolar organic dyes for DSSC application: A combined experimental and theoretical approach. *Org. Electron.* **2016**, *36*, 177–184. [[CrossRef](#)]
18. Mohankumar, V.; Pandian, M.S.; Ramasamy, P. Computational modelling on donor configuration for wide solar energy capture. *Mater. Lett.* **2018**, *219*, 216–219. [[CrossRef](#)]
19. Panicker, J.S.; Balan, B.; Soman, S.; Ghosh, T.; Nair, V.C. Thiophene-bithiazole based metal-free dye as DSSC sensitizer: Effect of co-adsorbents on photovoltaic efficiency. *J. Chem. Sci.* **2016**, *128*, 101–110. [[CrossRef](#)]
20. Richhariya, G.; Kumar, A.; Tekasakul, P.; Gupta, B. Natural dyes for dye sensitized solar cell: A review. *Renew. Sustain. Energy Rev.* **2017**, *69*, 705–718. [[CrossRef](#)]
21. Hosseinezhad, M.; Rouhani, S.; Gharanjig, K. Extraction and application of natural pigments for fabrication of green dye-sensitized solar cells. *Opto-Electron. Rev.* **2018**, *26*, 165–171. [[CrossRef](#)]
22. Gu, P.; Yang, D.Y.; Zhu, X.G.; Sun, H.; Li, J.T. Fabrication and characterization of dye-sensitized solar cells based on natural plants. *Chem. Phys. Lett.* **2018**, *693*, 16–22. [[CrossRef](#)]
23. Hamadianian, M.; Safaei, -G.J.; Hosseinpour, M.; Masoomi, R. Uses of new natural dye photosensitizers in fabrication of high potential dye-sensitized solar cells (DSSCs). *Mater. Sci. Semicond. Process.* **2014**, *27*, 733–739. [[CrossRef](#)]
24. Maiaugree, W.; Lowpa, S.; Towannang, M.; Rutphonsan, P.; Tangtrakarn, A.; Pimanpang, S.; Maiaugree, P.; Ratchapolthavisin, N.; Sang-aroon, W.; Jarernboon, W.; et al. A dye sensitized solar cell using natural counter electrode and natural dye derived from mangosteen peel waste. *Sci. Rep.* **2015**, *5*, 15230. [[CrossRef](#)] [[PubMed](#)]
25. Gómez-Ortíz, N.M.; Vazquez-Maldonado, I.A.; Perez-Espadas, A.R.; Mena-Rejon, G.J.; Azamar-Barrios, J.A.; Oskam, G. Dye-sensitized solar cells with natural dyes extracted from achiote seeds. *Sol. Energy Mater. Sol. Cells* **2010**, *94*, 40–44. [[CrossRef](#)]
26. Kumara, N.; Ekanayake, P.; Lim, A.; Liew, L.Y.C.; Iskandar, M.; Ming, L.C.; Senadeera, G.K.R. Layered co-sensitization for enhancement of conversion efficiency of natural dye sensitized solar cells. *J. Alloys Compd.* **2013**, *581*, 186–191. [[CrossRef](#)]
27. Ananth, S.; Vivek, P.; Arumanayagam, T.; Murugakoothan, P. Natural dye extract of lawsonia inermis seed as photo sensitizer for titanium dioxide based dye sensitized solar cells. *Spectrochim. Acta A Mol. Biomol. Spectrosc.* **2014**, *128*, 420–426. [[CrossRef](#)] [[PubMed](#)]
28. Mozaffari, S.A.; Saeidi, M.; Rahmanian, R. Photoelectric characterization of fabricated dye-sensitized solar cell using dye extracted from red Siahkooti fruit as natural sensitizer. *Spectrochim. Acta A Mol. Biomol. Spectrosc.* **2015**, *142*, 226–231. [[CrossRef](#)] [[PubMed](#)]

29. Sinha, K.; Saha, P.D.; Datta, S. Extraction of natural dye from petals of Flame of forest (*Butea monosperma*) flower: Process optimization using response surface methodology (RSM). *Dyes Pigm.* **2012**, *94*, 212–216. [[CrossRef](#)]
30. Chang, H.; Lo, Y.J. Pomegranate leaves and mulberry fruit as natural sensitizers for dye-sensitized solar cells. *Sol. Energy* **2010**, *84*, 1833–1837. [[CrossRef](#)]
31. Hao, S.C.; Wu, J.H.; Huang, Y.F.; Lin, J.M. Natural dyes as photosensitizers for dye-sensitized solar cell. *Sol. Energy* **2006**, *80*, 209–214. [[CrossRef](#)]
32. Kay, A.; Graetzel, M. Artificial photosynthesis. 1. Photosensitization of titania solar cells with chlorophyll derivatives and related natural porphyrins. *J. Phys. Chem.* **1993**, *97*, 6272–6277. [[CrossRef](#)]
33. Calogero, G.; Citro, I.; Crupi, C.; Marco, G.D. Absorption spectra and photovoltaic characterization of chlorophyllins as sensitizers for dye-sensitized solar cells. *Spectrochim. Acta A Mol. Biomol. Spectrosc.* **2014**, *132*, 477–484. [[CrossRef](#)] [[PubMed](#)]
34. Chava, R.K.; Lee, W.-M.; Oh, S.-Y.; Jeong, K.-U.; Yu, Y.-T. Improvement in light harvesting and device performance of dye sensitized solar cells using electrophoretic deposited hollow TiO₂ NPs scattering layer. *Sol. Energy Mater. Sol. Cells.* **2017**, *161*, 255–262. [[CrossRef](#)]
35. Chava, R.K.; Kang, M. Improving the photovoltaic conversion efficiency of ZnO based dye sensitized solar cells by indium doping. *J. Alloys Compd.* **2017**, *692*, 67–76. [[CrossRef](#)]
36. Song, P.; Li, Y.Z.; Ma, F.C.; Sun, M.T. Insight into external electric field dependent photoinduced intermolecular charge transport in BHJ solar cell materials. *J. Mater. Chem. C* **2015**, *3*, 4810–4819. [[CrossRef](#)]
37. Terranova, U.; Bowler, D.R. Self-consistent field method for natural anthocyanidin dyes. *J. Chem. Theory Comput.* **2013**, *9*, 3181–3188. [[CrossRef](#)]
38. Namuangruk, S.; Sirithip, K.; Rattanatwan, R.; Keawin, T.; Kungwan, N.; Sudyodsuk, T.; Promarak, V.; Surakhot, Y.; Jungstittiwong, S. Theoretical investigation of the charge-transfer properties in different meso-linked zinc porphyrins for highly efficient dye-sensitized solar cells. *Dalton Trans.* **2014**, *43*, 9166–9176. [[CrossRef](#)] [[PubMed](#)]
39. Ranjitha, S.; Rajarajan, G.; Gnanendra, T.S.; Anbarasan, P.M.; Aroulmoji, V. Structural and optical properties of Purpurin for dye-sensitized solar cells. *Spectrochim. Acta A Mol. Biomol. Spectrosc.* **2015**, *149*, 997–1008. [[CrossRef](#)] [[PubMed](#)]
40. Ren, P.F.; Zhang, Y.H.; Luo, Z.W.; Song, P.; Li, Y.Z. Theoretical and experimental study on spectra, electronic structure and photoelectric properties of three nature dyes used for solar cells. *J. Mol. Liq.* **2017**, *247*, 193–206. [[CrossRef](#)]
41. Qin, C.Y.; Clark, A.E. DFT characterization of the optical and redox properties of natural pigments relevant to dye-sensitized solar cells. *Chem. Phys. Lett.* **2007**, *438*, 26–30. [[CrossRef](#)]
42. Khadtare, S.S.; Ware, A.P.; Salunke-Gawali, S.; Jadkar, S.R.; Pingale, S.S.; Pathan, H.M. Dye sensitized solar cell with lawsone dye using a ZnO photoanode: Experimental and TD-DFT study. *RSC Adv.* **2015**, *5*, 17647–17652. [[CrossRef](#)]
43. Kang, G.-J.; Song, C.; Ren, X.-F. Charge transfer enhancement in the D- π -A type porphyrin dyes: A density functional theory (DFT) and time-dependent density functional theory (TD-DFT) study. *Molecules* **2016**, *21*, 1618. [[CrossRef](#)] [[PubMed](#)]
44. Ramasamy, E.; Lee, J. Ferrocene-derivatized ordered mesoporous carbon as high performance counter electrodes for dye-sensitized solar cells. *Carbon* **2010**, *48*, 3715–3720. [[CrossRef](#)]
45. Hohenberg, P.; Kohn, W. Inhomogeneous Electron Gas. *Phys. Rev.* **1964**, *136*, B864–B871. [[CrossRef](#)]
46. Lee, C.; Yang, W.; Parr, R.G. Development of the Colle-Salvetti correlation-energy formula into a functional of the electron density. *Phys. Rev. B* **1988**, *37*, 785–789. [[CrossRef](#)]
47. Becke, A.D. Density-functional exchange-energy approximation with correct asymptotic behavior. *Phys. Rev. A* **1988**, *38*, 3098–3100. [[CrossRef](#)]
48. Becke, A.D. Density-functional thermochemistry. I. The effect of the exchange-only gradient correction. *J. Chem. Phys.* **1992**, *96*, 2155–2160. [[CrossRef](#)]
49. Stratmann, R.E.; Scuseria, G.E.; Frisch, M.J. An efficient implementation of time-dependent density-functional theory for the calculation of excitation energies of large molecules. *J. Chem. Phys.* **1998**, *109*, 8218–8224. [[CrossRef](#)]
50. Yanai, T.; Tew, D.P.; Handy, N.C. A new hybrid exchange–correlation functional using the Coulomb-attenuating method (CAM-B3LYP). *Chem. Phys. Lett.* **2004**, *393*, 51–57. [[CrossRef](#)]

51. Perdew, J.P.; Burke, K.; Wang, Y. Generalized gradient approximation for the exchange-correlation hole of a many-electron system. *Phys. Rev. B* **1996**, *54*, 16533–16539. [[CrossRef](#)]
52. Adamo, C.; Barone, V. Exchange functionals with improved long-range behavior and adiabatic connection methods without adjustable parameters: The mPW and mPW1PW models. *J. Chem. Phys.* **1998**, *108*, 664–675. [[CrossRef](#)]
53. Perdew, J.P.; Burke, K.; Ernzerhof, M. Generalized gradient approximation made simple. *Phys. Rev. Lett.* **1996**, *77*, 3865–3868. [[CrossRef](#)] [[PubMed](#)]
54. Ordon, P.; Tachibana, A. Investigation of the role of the C-PCM solvent effect in reactivity indices. *J. Chem. Sci.* **2005**, *117*, 583–589. [[CrossRef](#)]
55. Alberto, M.E.; Comuzzi, C.; Thandu, M.; Adamo, C.; Russo, N. 22π -Electrons [1.1.1.1.1] pentaphyrin as a new photosensitizing agent for water disinfection: Experimental and theoretical characterization. *Theor. Chem. Acc.* **2016**, *135*, 29. [[CrossRef](#)]
56. Mazzone, G.; Alberto, M.E.; De Simone, B.C.; Marino, T.; Russo, N. Can Expanded Bacteriochlorins Act as Photosensitizers in Photodynamic Therapy? Good News from Density Functional Theory Computations. *Molecules* **2016**, *21*, 288. [[CrossRef](#)]
57. Zong, H.; Wang, J.C.; Mu, X.J.; Xu, X.F.; Li, J.; Wang, X.Y.; Long, F.X.; Wang, J.X.; Sun, M.T. Physical mechanism of photoinduced intermolecular charge transfer enhanced by fluorescence resonance energy transfer. *Phys. Chem. Chem. Phys.* **2018**, *20*, 13558–13565. [[CrossRef](#)]
58. Li, Q.J.; Wang, J.G.; Ding, Q.Q.; Chen, M.D.; Ma, F.C. Coupling effect on charge-transfer mechanism of surface-enhanced resonance Raman scattering. *J. Raman Spectrosc.* **2017**, *48*, 560–569. [[CrossRef](#)]
59. Li, Y.Z.; Xu, B.B.; Song, P.; Ma, F.C.; Sun, M.T. J D–A– π –A system: Light harvesting, charge transfer, and molecular designing. *Phys. Chem. C* **2017**, *121*, 12546–12561. [[CrossRef](#)]
60. Li, Y.Z.; Sun, C.F.; Song, P.; Ma, F.C.; Yang, Y.H. Tuning the electron-transport and electron-accepting abilities of dyes through introduction of different π -conjugated bridges and acceptors for dye-sensitized solar cells. *ChemPhysChem* **2017**, *18*, 366–383. [[CrossRef](#)] [[PubMed](#)]
61. Frisch, M.J.; Trucks, G.W.; Schlegel, H.B.; Scuseria, G.E.; Robb, M.A.; Cheeseman, J.R.; Scalmani, G.; Barone, V.; Mennucci, B.; Petersson, G.A.; et al. G09. Available online: <http://gaussian.com/glossary/g09/> (accessed on 5 June 2015).
62. Al-Alwani, M.A.M.; Mohamad, A.B.; Kadhun, A.A.H.; Ludin, N.A. Effect of solvents on the extraction of natural pigments and adsorption onto TiO₂ for dye-sensitized solar cell applications. *Spectrochim. Acta A Mol. Biomol. Spectrosc.* **2015**, *138*, 130–137. [[CrossRef](#)] [[PubMed](#)]
63. Suyitno, S.; Saputra, T.J.; Supriyanto, A.; Arifin, Z. Stability and efficiency of dye-sensitized solar cells based on papaya-leaf dye. *Spectrochim. Acta A Mol. Biomol. Spectrosc.* **2015**, *148*, 99–104. [[CrossRef](#)] [[PubMed](#)]
64. Sengupta, D.; Mondal, B.; Mukherjee, K. Visible light absorption and photo-sensitizing properties of spinach leaves and beetroot extracted natural dyes. *Spectrochim. Acta A Mol. Biomol. Spectrosc.* **2015**, *148*, 85–92. [[CrossRef](#)]
65. Manoharan, S.; Wu, J.J.; Anandan, S. Synthesis of cyanovinyl thiophene with different acceptor containing organic dyes towards high efficient dye sensitized solar cells. *Dyes Pigments* **2016**, *133*, 222–231. [[CrossRef](#)]
66. Nazeeruddin, M.K.; Kay, A.; Rodicio, I.; Humphry-Baker, R.; Mueller, E.; Liska, P.; Vlachopoulos, N.; Graetzel, M. Conversion of light to electricity by cis-X₂bis(2,2'-bipyridyl-4,4'-dicarboxylate)ruthenium(II) charge-transfer sensitizers (X = Cl-, Br-, I-, CN-, and SCN-) on nanocrystalline titanium dioxide electrodes. *J. Am. Chem. Soc.* **1993**, *115*, 6382–6390. [[CrossRef](#)]
67. Tian, H.; Yang, X.; Cong, J.; Chen, R.; Teng, C.; Liu, J.; Hao, Y.; Wang, L.; Sun, L. Effect of different electron donating groups on the performance of dye-sensitized solar cells. *Dyes Pigments* **2010**, *84*, 62–68. [[CrossRef](#)]
68. Liu, X.R.; He, R.X.; Shen, W.; Li, M. Molecular design of donor–acceptor conjugated copolymers based on C-, Si- and N-bridged dithiophene and thienopyrroledione derivatives units for organic solar cells. *J. Power Sources* **2014**, *245*, 217–223. [[CrossRef](#)]
69. Grätzel, M. Recent Advances in Sensitized Mesoscopic Solar Cells. *Acc. Chem. Res.* **2009**, *42*, 1788–1798. [[CrossRef](#)] [[PubMed](#)]

